

Detail Across Scales: Multi-Scale Enhancement for Full Spectrum Neural Representations

Yuan Ni,^{1, 2,*} Zhantao Chen,^{1, 2, 3} Cheng Peng,² Rajan Plumley,^{1, 2, 4}
 Chun Hong Yoon,¹ Jana B. Thayer,¹ and Joshua J. Turner^{1, 2, †}

¹*SLAC National Accelerator Laboratory, Menlo Park, CA 94025, USA.*

²*Stanford Institute for Materials and Energy Sciences, Stanford University, Stanford, CA 94305, USA.*

³*Walker Department of Mechanical Engineering, The University of Texas at Austin, Austin, Texas 78712, USA.*

⁴*Department of Physics, Carnegie Mellon University, Pittsburgh, PA 15213, USA.*

Abstract Implicit neural representations (INRs) have emerged as a compact and parametric alternative to discrete array-based data representations, encoding information directly in neural network weights to enable resolution-independent representation and memory efficiency. However, existing INR approaches, when constrained to compact network sizes, struggle to faithfully represent the multi-scale structures, high-frequency information, and fine textures that characterize the majority of scientific datasets. To address this limitation, we propose WIEN-INR, a wavelet-informed implicit neural representation that distributes modeling across different resolution scales and employs a specialized kernel network at the finest scale to recover subtle details. This multi-scale architecture allows for the use of smaller networks to retain the full spectrum of information while preserving the training efficiency and reducing storage cost. Through extensive experiments on diverse scientific datasets spanning different scales and structural complexities, WIEN-INR achieves superior reconstruction fidelity while maintaining a compact model size. These results demonstrate WIEN-INR as a practical neural representation framework for high-fidelity scientific data encoding, extending the applicability of INRs to domains where efficient preservation of fine detail is essential.

Keywords: Neural Data Compression, Implicit Neural Representation (INRs), Wavelet Transformation and Multi-resolution Analysis, X-ray and Neutron scattering experiments, Machine Learning.

I. INTRODUCTION

As scientific facilities generate increasingly massive datasets at accelerating rates, storage and analysis of voxel-based data representations become unsustainable, creating an urgent need for frameworks that enable scalable analytical utility while maintaining compact memory requirements [4, 5]. Implicit neural representations (INRs) have established a new paradigm for data representation by encoding information as neural network weights [6]. INRs offer several distinctive advantages over rasterized formats and traditional codecs: memory efficiency that scales with signal complexity rather than resolution [7–9]; continuous functional fitting and differentiability with gradient access; resolution independence and region-of-interest (ROI) decoding through coordinate-based queries [3, 10]. All these features are well aligned with a data-driven compression-and-analysis scientific workflow.

However, deploying INRs for high-stakes scientific data—where high-fidelity representation is essential—requires that they simultaneously (i) preserve both coarse and fine structures, (ii) capture high-frequency details and textures, and (iii) be computationally scalable and remain storage efficient. Compact networks often suffer from a low-frequency bias that tends to capture smooth components before high-frequency details

[1, 3], while larger models capture fine structure but undermine compactness representation. This trade-off resonates with rate-distortion theory in signal processing [11] : the minimum number of bits (rate) required to represent data depends on how much information can be altered or discarded without exceeding a specified error threshold. Such rates are in turn determined by network size, weight quantization, and entropy coding [8, 12]. In the ideal case, increasing network size guarantees universal approximation [13], meaning that sufficiently large models can represent any measurable function arbitrarily well. In practice, however, this theoretical capacity faces two significant constraints. First, existing INR architectures are often not parameter-efficient, implying that smaller networks could achieve the same representational power. Second, simply enlarging the network does not always ensure convergence to the desired accuracy, particularly for fine-scale or high-frequency structures which are often more difficult to capture accurately. When such high-frequency components contain critical physical information, such as the speckles in X-ray scattering, omitting those components leads to substantial reconstruction errors. These limitations highlight the need for compact, full-spectrum representations that preserve both global structure and localized detail, allowing small networks to achieve high fidelity without loss of efficiency.

In this paper, we present the Wavelet Implicit Enhancement Network (WIEN-INR), an INR-based compressive framework that encodes multi-resolution wavelet coefficients and integrates a compact enhancement module to enhance the representation capability of any coordinate-based INRs. The proposed design

* yn754@slac.stanford.edu

† joshuat@slac.stanford.edu

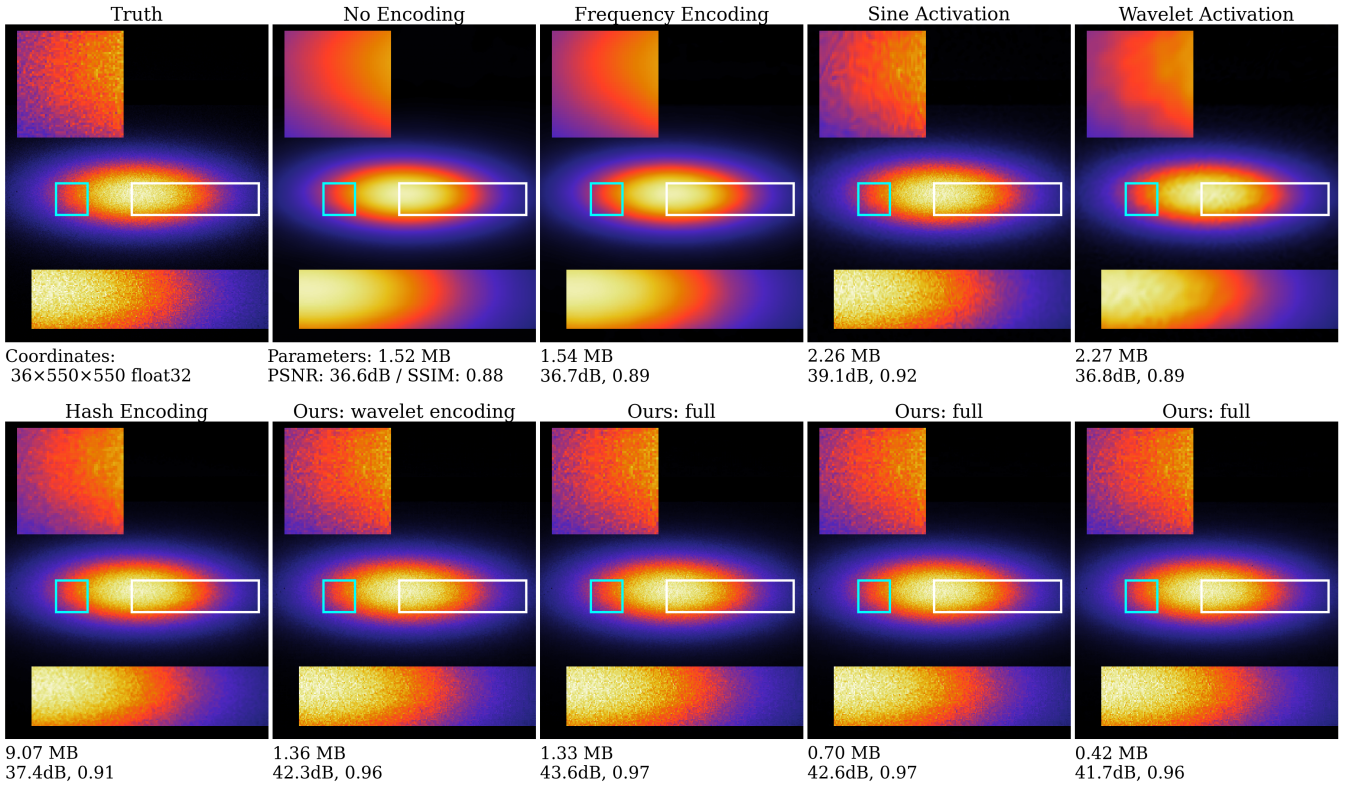


FIG. 1. Efficient implicit neural representations preserve high-frequency detail. Comparison of implicit neural representations of raw volumetric data ($36 \times 550 \times 550$, float32) collected from a high-resolution wide-angle X-ray scattering experiment from a Cu₃Au experiment. Each trained network serves as a compressed surrogate for the original volume: instead of storing the raw voxel array, the information is encoded in the network weights. The figure shows a specific slice reconstructed at inference by querying the trained INRs with the corresponding spatial coordinates and using the network outputs as pixel intensities. In all cases, the network size is smaller than the raw data representation. One unique challenge for scattering dataset is that speckles constitute the signal of interest, whereas in many other imaging fields they are treated as noise and removed. Insets zoom into regions of high-speckle intensity, highlighting the superior ability of our method to capture fine details and textures. Competing INRs either over-smooth the data (Frequency Encoding [1], Wavelet Activation[2]) or produce unphysical textures (Sine activation [3]), whereas our methods preserves fine-scale structures and achieves higher PSNR/SSIM with fewer parameters.

mitigates the low-frequency bias of standard INRs through a frequency-divided representation, ensures full-spectrum approximation via multi-resolution modeling, and extends representational capacity by introducing a novel INR enhancement architecture that enables the preservation of high-frequency details with a small network. We demonstrate that WIEN-INR achieves significant improvements in compressive neural representation—across accuracy, training time, spectral fidelity, texture preservation, and robustness—which collectively address several challenges faced by INR-based methods in efficiently representing scientific data. We showcase the effectiveness of the proposed framework across a wide range of complex scientific datasets, including high-resolution X-ray diffraction, 4D inelastic neutron spectroscopy, and ultra-fast X-ray scattering, demonstrating its robustness across domains of vastly different scales and modalities. We also discuss the robustness of using different hyperparameter choices and network

configurations. Finally, we discuss how INR-based representations open up new possibilities for scientific data storage, analysis and discovery.

II. BACKGROUND

Our approach is motivated by two key observations. First, achieving representations that faithfully preserve the full frequency spectrum while remaining compact requires architectures that can effectively capture meaningful information without discarding scientifically relevant detail. Second, compact networks must be endowed with mechanisms that enhance their representational capacity. As illustrated in Fig.1, existing INR frameworks, when constrained to a small parameter size, often over-smooth fine details or introduce unphysical textures, as exemplified by a representative raw X-ray speckle dataset. This

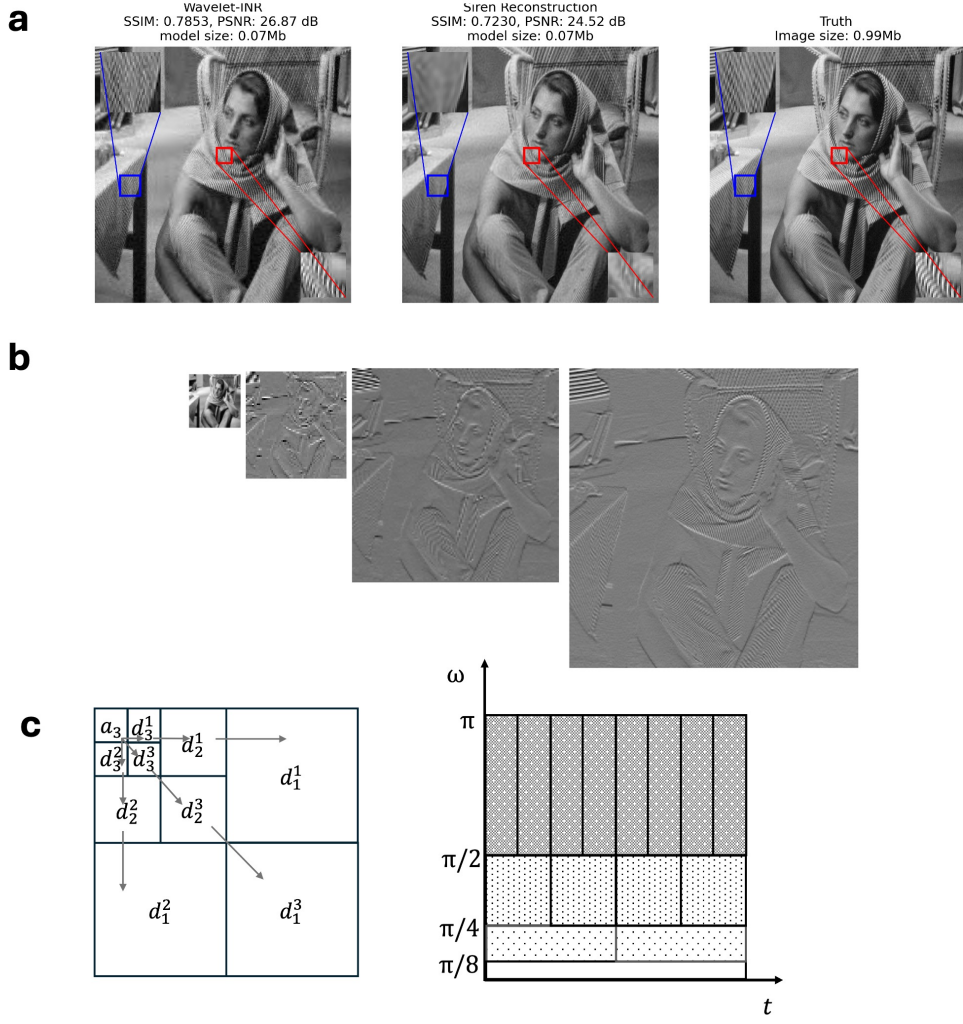


FIG. 2. Multi-resolution wavelet decomposition with implicit neural representations. **a** Neural Representation of the Barbara image using different INR approaches. Left: Separate INRs for each DWT sub-band. Center: A single network representing all frequency bands jointly. Right: Ground truth image. With the same total number of network parameters, the left decomposition assigns more representational capacity to high-frequency bands, yielding a sharper reconstruction with enhanced fine details. **b**, Example wavelet coefficients of the Barbara image, showing approximation coefficients \mathbf{a}_3 and detail coefficients $\mathbf{d}_3, \mathbf{d}_2$, and \mathbf{d}_1^1 (from left to right). **c, left**, Schematic of a two-dimensional wavelet transform, where the lowest-frequency approximation sub-band (\mathbf{a}_3) occupies the top-left quadrant, and progressively higher-frequency detail sub-bands appear toward the bottom right. Within each scale j , the three detail sub-bands ($\mathbf{d}_j^1, \mathbf{d}_j^2, \mathbf{d}_j^3$) capture horizontal, vertical, and diagonal orientations, respectively. **c, right**, Corresponding tiling of the time-frequency plane. Each successive scale approximately halves the bandwidth in the frequency domain, with scale j responding primarily to the octave $[\pi/2^j, \pi/2^{j-1}]$, subject to overlap due to the non-ideal frequency localization of practical wavelets.

is also evident from the demonstration using the Barbara image (Fig. 2).

a. INR The central idea behind Implicit Neural Representation (INR) is to convert explicit information into implicit model weights through unsupervised training. Specifically, given an input coordinate $\mathbf{x} \in \mathbb{R}^p$, we are interested in learning a function that maps \mathbf{x} to a quantity of interest $\mathbf{y} \in \mathbb{R}^N$. Such a mapping can be approximated by a neural network, typically a Multilayer Perceptron (MLP), $\varphi_\omega(\mathbf{x})$ parametrized by the weights

ω :

$$\varphi_\omega : \Omega \subset \mathbb{R}^p \longrightarrow \mathbb{R}^N, \quad \mathbf{x} \mapsto \varphi_\omega(\mathbf{x}),$$

where p is the input dimension and N is the output dimension (e.g., $N = 1$ for scalar fields, $N = 3$ for RGB values).

To query a multi-dimensional tensor $\mathbf{I} \in \mathbb{R}^{D_1 \times D_2 \times \dots \times D_p}$, we evaluate the network on a coordinate grid. We denote by

$$\mathcal{I} = \{(i_1, \dots, i_p) : 1 \leq i_j \leq D_j\}$$

the full set of index tuples. Each index $(i_1, \dots, i_p) \in \mathcal{I}$ corresponds to a normalized coordinate $\mathbf{x}_{i_1, \dots, i_p} \in [-1, 1]^p$ and a tensor value $\mathbf{I}[i_1, \dots, i_p] \in \mathbb{R}^N$.

The INR is trained to minimize the discrepancy between its predictions and the ground-truth tensor values at all discrete coordinates:

$$\min_{\omega} \sum_{(i_1, \dots, i_p) \in \mathcal{I}} \mathcal{L}(\varphi_{\omega}(\mathbf{x}_{i_1, \dots, i_p}), \mathbf{I}[i_1, \dots, i_p]), \quad (1)$$

where \mathcal{L} denotes a suitable loss function. In practice, this full-sum objective is optimized over mini-batches by sampling from \mathcal{I} . The training objective in Eq. (1) is conceptually straightforward, yet convergence is not guaranteed by the objective alone [3, 14].

b. Wavelet transformations and multi-resolution analysis The question of identifying which features can be safely removed without affecting reconstruction quality is highly non-trivial, and what seems like “noise” to a model may be signal to a researcher [15]. A partial answer lies in selecting an appropriate analysis window—such as a block size or time interval that ensures meaningful patterns in the data are effectively captured [16]. This choice involves a tradeoff: smaller windows allow for detection of localized, high-frequency phenomena or “anomalies,” whereas larger windows tend to smooth over these details and are better suited for identifying broader, low-frequency trends [16]. From signal processing, we know that methods that rely on assumptions of stationarity or ergodicity over large windows (e.g., Fourier analysis) tend to obscure transient or localized phenomena, particularly when the underlying data are random or nonstationary [16, 17].

Wavelet theory and multiscale analysis offer a compelling solution to this tradeoff by enabling the simultaneous examination of both local anomalies and global trends. In the wavelet domain, the coefficients provide a hierarchical description of the signal: some capture long-range correlations with narrow frequency bands, while others represent short-term variations associated with wide frequency bands. This multiscale representation inherently allows for a flexible balance between resolution in time (or space) against resolution in frequency (or momentum). An illustration of the wavelet transform and its time–frequency tiling is shown in Fig. 2. Additional details on the wavelet transform are provided in Appendix B1.

This multiscale capability is particularly desirable in physics data analysis, where phenomena of interest often manifest across a range of spatial or temporal scales.

c. Beating the low-frequency bias. Inspired by wavelet theory, we explore a hierarchical INR design that encodes the wavelet coefficients of the data instead of working with the raw space. In principle, a sufficiently expressive coordinate MLP could emulate multiscale transforms (and even surpass them) by virtue of universal approximation. In practice, however, optimization dynamics make this inefficient: standard INRs

exhibit a well-documented spectral bias—they fit low frequencies first and struggle to recover high-frequency structure—so convergence on fine detail is slow or requires substantially larger models [1, 3].

The INR community has developed many notable techniques to mitigate the network’s inherent spectral bias. A few approaches include positional encoding [1, 18], which maps input coordinates to higher-dimensional features, hash encoding [9] which introduced a efficient multi-resolution grids of trainable features for compact representation, and alternative activation functions such as sinusoidal or wavelet activations as in SIREN [3] and WIRE [2]. Additionally, more recent methods focus on improving model architectures to better capture fine details and a wider range of frequencies, such as INCODE, MFN and FR [19–21]. While preparing this manuscript, Yu et al. [22] independently proposed CF-INR, which also directly encode the wavelet coefficients for INR learning. Their approach uses a single-level Haar decomposition with self-evolving parameters, whereas WIEN-INR adopts a multi-level wavelet pyramid with a dedicated enhancement module designed for compact, high-fidelity data representation.

III. WIEN-INR: LEARNING THE FINE DETAILS

The design of WIEN-INR is guided by two principles. First, rate–distortion can be improved by operating in a domain that better decouples and de-correlates information across scales. We achieve this by applying a wavelet transform to partition the signal into different frequency bands across scales. Second, compact coordinate-based MLPs can be endowed with additional representational power through a lightweight enhancement module, enabling them to capture subtle details without inflating network size. Both components are modular: the wavelet transform acts as a preprocessing step, and the enhancement module can be integrated with any coordinate-based INRs.

a. A multi-resolution preprocess. The first step in WIEN-INR is to apply a wavelet transform to the input tensor \mathbf{I} , decomposing it into frequency bands that are better de-correlated. The time–frequency localization property of the wavelet transform helps alleviate the low-frequency bias in compressive INRs by isolating high-frequency details into dedicated sub-bands. We denote the wavelet coefficients of general p -dimensional data with approximation coefficients denoted by \mathbf{a}_J , and j -th detail scale with direction i as $\mathbf{d}_j^i, 1 \leq j \leq J, 1 \leq i \leq 2^p - 1$. A straightforward approach to operate in the wavelet space is to apply a discrete wavelet transform (DWT) to the signal and then train separate compressive INRs to model each sub-band independently, and finally reconstruct the signal using the inverse discrete wavelet transform. Other transformation choices are discussed in

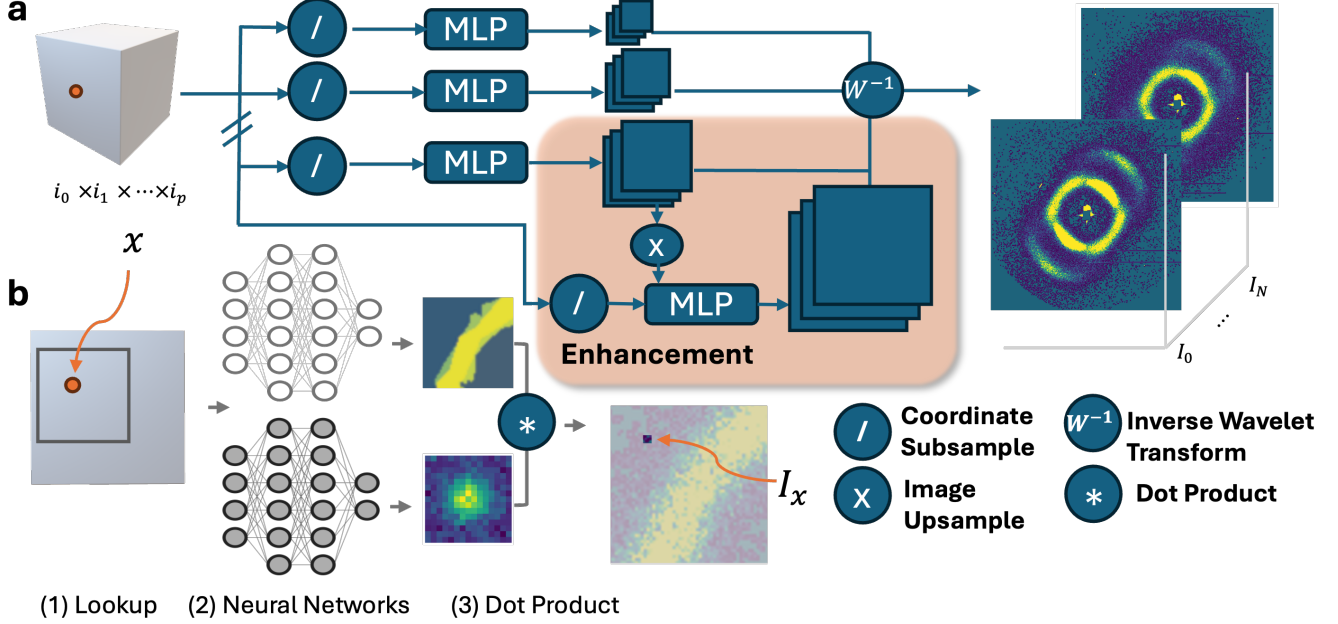


FIG. 3. **Schematic of the WIEN-INR architecture.** **a.** p -dimensional input coordinates (e.g., detector coordinate $\mathbf{x} = [i, j]$) are passed to separate INRs, each trained independently or progressively to predict the DWT coefficient at its resolution scale (see Sec. III 0 a for details). In the progressive setting, enhancement modules recover the next scales from coarser scales. **b.** In the enhancement module, for a given coordinate \mathbf{x} , (1) a local neighborhood of voxels centered at \mathbf{x} is extracted; (2) The local neighborhood is input to two INRs, one providing a coarse-scale approximation and the other a learnable refinement; (3) Apply dot product to the outputs of these two networks yield the scalar intensity $I(\mathbf{x})$; This operation is rasterized over all coordinates in the domain to reconstruct the signal. Finally, output from the networks are transformed back to the true signal domain (e.g., a batch N of diffraction patterns \mathbf{I}_N). This process is applicable to high dimensional outputs.

Appendix B1. The training process is the following,

$$\min_{\omega_j, \omega_J} \sum_{j=1}^{J-1} \sum_{i=1}^{2^p-1} \left\| \varphi_{\omega_j}^i - \mathbf{d}_j^i \right\|^2 + \left\| \varphi_{\omega_J} - \mathbf{a}_J \right\|^2. \quad (2)$$

Each NN $\varphi_{\omega_j}^i : \mathbf{x} \mapsto \mathbb{R}^N$ is typically parameterized as an MLP that maps spatial coordinates $\mathbf{x} \in \Omega_j$ at the appropriate resolution to the corresponding wavelet coefficient.

However, this naive formulation suffers from three major drawbacks: (1) it requires storing and training a separate network for each sub-band, leading to redundancy in both parameters and training time, (2) it ignores the strong statistical correlations of the wavelet coefficients across scales and orientations, which are well-exploited in wavelet theory and zerotree coding [16, 17], and (3) generic INR architectures struggle to converge for the finest scale due to their limited representational capacity when constrained to small network sizes. These noted shortcomings call for a more tailored architecture to handle the compression of the finest band, and ultimately, to produce the improved quality decoded data.

b. Model correlation with a shared INR per scale. Induced by the geometric image regularity [16], the significant coefficients in \mathbf{d}_j^i tend to be aggregated along contours or in textured regions. Indeed, wavelet coeffi-

cients have a large amplitude where the signal has sharp transitions. At each scale and for each orientation, a wavelet image coder can take advantage of the correlation between neighboring wavelet coefficient amplitudes, referred to as *intraband correlation*. Note that taking advantage of this intrascale amplitude correlation is an important source of improvement for traditional compression techniques, such as in JPEG-2000 compression [23].

Taking this into account, instead of using independent INRs for each of the $2^p - 1$ directions of i , we can use a single INR with an output dimension of $2^p - 1$ such that it encodes information from all directions simultaneously. Specifically, we train a single φ_{ω_j} for the scale j such that $\varphi_{\omega_i} : \mathbf{x} \mapsto \mathbb{R}^{N(2^p-1)}$. And the optimization problem becomes:

$$\min_{\omega_j, \omega_J} \sum_{j=1}^{J-1} \left\| \varphi_{\omega_j} - (\mathbf{d}_j^1, \dots, \mathbf{d}_j^{2^p-1}) \right\|^2 + \left\| \varphi_{\omega_J} - \mathbf{a}_J \right\|^2 \quad (3)$$

Ideally, by adjusting the frequency bias of each φ_{ω_i} — for example via the frequency scaling parameter in SIREN or frequency encoding — we can align each network with the frequency range for scale j it is intended to model (e.g., see 2). We call this new formulation of combining wavelet transform theory with a new INR architecture (3) **WAVELET-INR**.

c. Enhancement module. From our experiments, we observe that the finest detail band (approximately corresponding to frequency $\omega \in [\pi/2, \pi]$) is particularly challenging for a small INR to represent. While one possible remedy might be to further decompose this band (e.g., using wavelet packets [24]), we argue that the difficulty does not stem primarily from frequency bias. Instead, it arises because generic INRs — especially in their compressive form — struggle to effectively capture and reproduce such fine-scale textures. To overcome this limitation, we introduce a tailored INR-based neural architecture that increases representational capacity for any coordinate-based INRs without incurring a significant increase in model size.

This is achieved by inferring finer-scale details conditioned on coarser-scale representations: For each fixed orientation i , suppose we can approximate scale j with a light-weight INR $\varphi_j^i : \Omega_j \rightarrow \mathbb{R}^N$. Then for the next finer scale ($j-1$) of the same i , the coefficient can be approximated by super-resolving φ_j^i onto the next scale Ω_{j-1} ,

$$\varphi_{j-1}^i : \Omega_{j-1} \rightarrow \mathbb{R}^N, \text{ such that } \varphi_{j-1}^i(\mathbf{x}) = \varphi_j^i(\mathbf{x}). \quad (4)$$

This upsampling operation is possible due to the continuity of the INR, and can be done recursively up to the finest detail Ω_1 . However, these upsampled networks do not contain higher frequency information beyond the scale on which they were trained. Instead, they provide an approximate prediction of the next scale, serving primarily as a geometric prior to guide the encoding of finer details — similar in spirit to zero-tree coding [17].

To super-resolve the fine details, we introduce a light-weight predictor network using MLP that acts as a local learnable deconvolution operator. Specifically, for a fixed orientation i , we train a predictor $P_{j \rightarrow j-1}^i : \Omega_{j-1} \rightarrow \mathbb{R}^{Nr_{j-1}^p}$ to super-resolve the coarser upsampled predictions. It takes as input a coordinate $\mathbf{x} \in \Omega_{j-1}$ and outputs a kernel of size $r \times r$ (or r^p in p dimensions) for each output dimension. Conceptually, this kernel corresponds to a local receptive field centered at \mathbf{x} . During training, for each coordinate \mathbf{x} in Ω_{j-1} , we: (1) Extract an $r \times r$ patch from the upsampled coarser-scale INR prediction φ_j^i , centered at \mathbf{x} . (2) Apply the kernel produced by the predictor $P_{j \rightarrow j-1}^i(\mathbf{x})$ to this patch (via the inner product). (3) Match the resulting scalar prediction to the true wavelet coefficient $\mathbf{d}_{j-1}^i(\mathbf{x})$. The training objective is therefore:

$$\min_{\xi} \sum_{\mathbf{x} \in \Omega_{i-1}} \|\mathbf{d}_{j-1}^i - \langle \varphi_{j-1}^i(\mathcal{N}_{\nabla}(\mathbf{x})), P_{j \rightarrow j-1, \xi}^i(\mathbf{x}) \rangle\|^2, \quad (5)$$

where $\mathcal{N}_r(\mathbf{x})$ denotes the $r \times r$ neighborhood of \mathbf{x} in the upsampled coarse prediction. A schematic view of this structure can be found in Fig 3.

This idea is reminiscent of a progressive refinement, where a network learns to predict the distortion between a coarse approximation and the true signal [25]. Note the enhancement module is stand-alone and can be

applied to any coordinate-based INR. We also test an alternative approach that uses a residual network to model the difference; details are provided in Appendix A1.

IV. EXPERIMENTS

We demonstrate that our proposed method achieves accurate representation that preserves fine-scale details and textures while maintaining a small network size, delivering strong rate-distortion performance.

a. Architecture and training of INR For the subnetworks that represent each scale (i.e., $\{\psi_{\omega_j}, \psi_{\omega_J}\}$), we use independent SIREN networks with three hidden layers, where the sine layer frequencies are varied across scales, which controls the distribution of frequencies the network represents. The subnetwork size is controlled solely by adjusting the hidden layer dimensions. The enhancement kernel network is also implemented using a SIREN, with tunable hidden layer width but fixed frequency parameters $\omega_0 = 30$ for the first layer and $\omega = 30$ for the hidden layers. We choose to apply the enhancement structure to the finest detail band (i.e., \mathbf{d}_2 level to the \mathbf{d}_1 level) and we use SIREN for lower frequency scales. This choice is data-dependent (e.g., distribution of information across wavelet bands), but we found it sufficient for all evaluated scientific datasets, where the most challenging information to compress resides in the finest details. In practice, the enhancement network can be applied at any scale.

We implemented our framework on NVIDIA A100 GPUs with 40 GB memory. To optimize inference and decompression, all trained model weights are stored in half precision (2 bytes per entry). For training stability, we maintain a master copy of the parameters in full precision and use mixed-precision updates.

TABLE I. Model parameters and their ranges in our results.

Parameter	Value
Number of scales (J)	1 to 4
Enhancement network window size	$(2^1 + 1)^p$ to $(2^3 + 1)^p$
Type of wavelet	Haar, Daubechies, Coiflet, Symlet, Biorthogonal
Hidden layer width per subnetwork	24 to 1024

b. Improved rate-distortion. We quantify reconstruction accuracy using peak signal-to-noise ratio (PSNR), structural similarity index (SSIM), and pixel-wise correlation. Compression rate is defined as

$$\text{Compression Ratio} = \frac{\text{Size of network weights}}{\text{Size of original tensor}}.$$

We minimize the ℓ_2 loss in Eq. (1). Since the loss is separable across scales, we train each subnetwork independently, one scale at a time. During training, we fix a

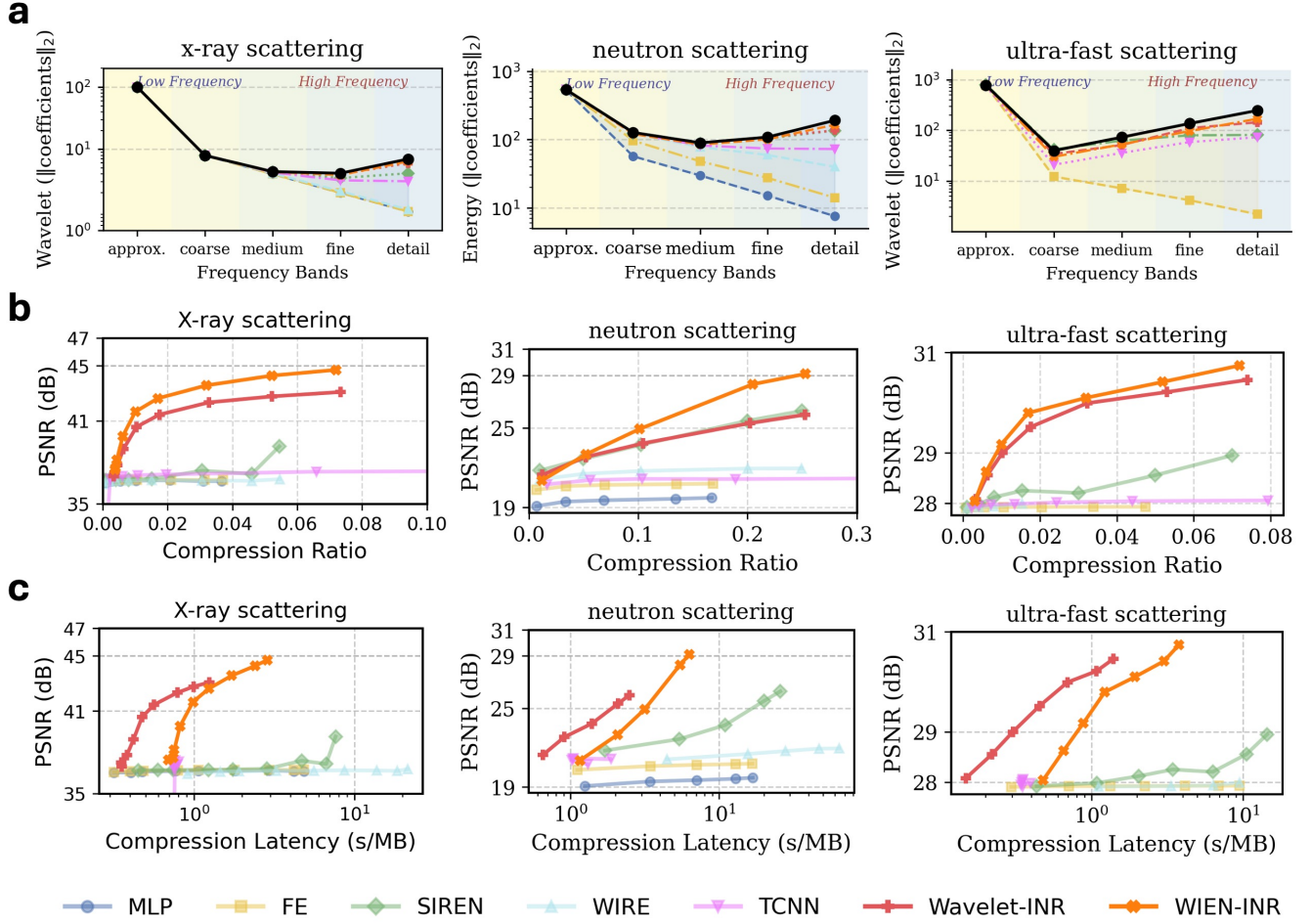


FIG. 4. Improved rate-distortion. **a**, Preservation of wavelet coefficient magnitudes using $J = 4$ scales. We plot the ℓ_2 norm of reconstructed DWT coefficients across sub-bands, quantifying how well each method maintains the distribution of information from coarse to fine scales. While baselines remain close to the ground truth at coarse levels (*a* and d_1) but deviate at finer scales, WIEN-INR closely follows the true DWT distribution (black line), demonstrating robust recovery of fine-scale content. **b**, Rate-distortion comparison across three scientific datasets, showing compression ratio versus PSNR. At convergence, WIEN-INR consistently achieves higher PSNR than other INR methods at the same compression ratio, indicating that WIEN-INR achieves more accurate reconstructions with fewer parameters. **c**, Encoding efficiency under the same setting as in **b**, with encoding time (latency) recorded and plotted against PSNR. For equivalent PSNR, WIEN-INR requires less encoding time, highlighting its advantage in both fidelity and efficiency.

target compression level and allocate the total parameter budget across scales according to the intrinsic data dimensionality: coarser scales are assigned smaller SIREN subnetworks with reduced hidden features, while finer scales receive larger subnetworks to better capture detail.

We evaluate WIEN-INR on three distinct scientific datasets, including wide-angle X-ray scattering, Neutron scattering [27] and ultra-fast X-ray scattering [26], each probing different physical properties. A detailed description of the datasets, including their physical origins and experimental objectives, is provided in Appendix C1. For comparison, we benchmark against FE [1], SIREN [3], WIRE [2], and TCNN [9], each representing a com-

pact network design that incorporates frequency or multi-resolution considerations, either through input encoding, activation functions, or architectural structure. Within the WIEN-INR's MLP modules, we adopt SIREN, as it consistently achieved the best standalone performance across the scientific datasets examined in this work.

Figure 4 presents the main result, showing our method consistently achieves superior rate-distortion performance compared to all benchmarks. Additionally, we compare pixel-wise differences and correlation with ground truth (Fig. 6).

c. Choice of the Wavelet and Number of Scales. WIEN-INR is robust to hyperparameters, including wavelet basis, decomposition level J , and refinement win-

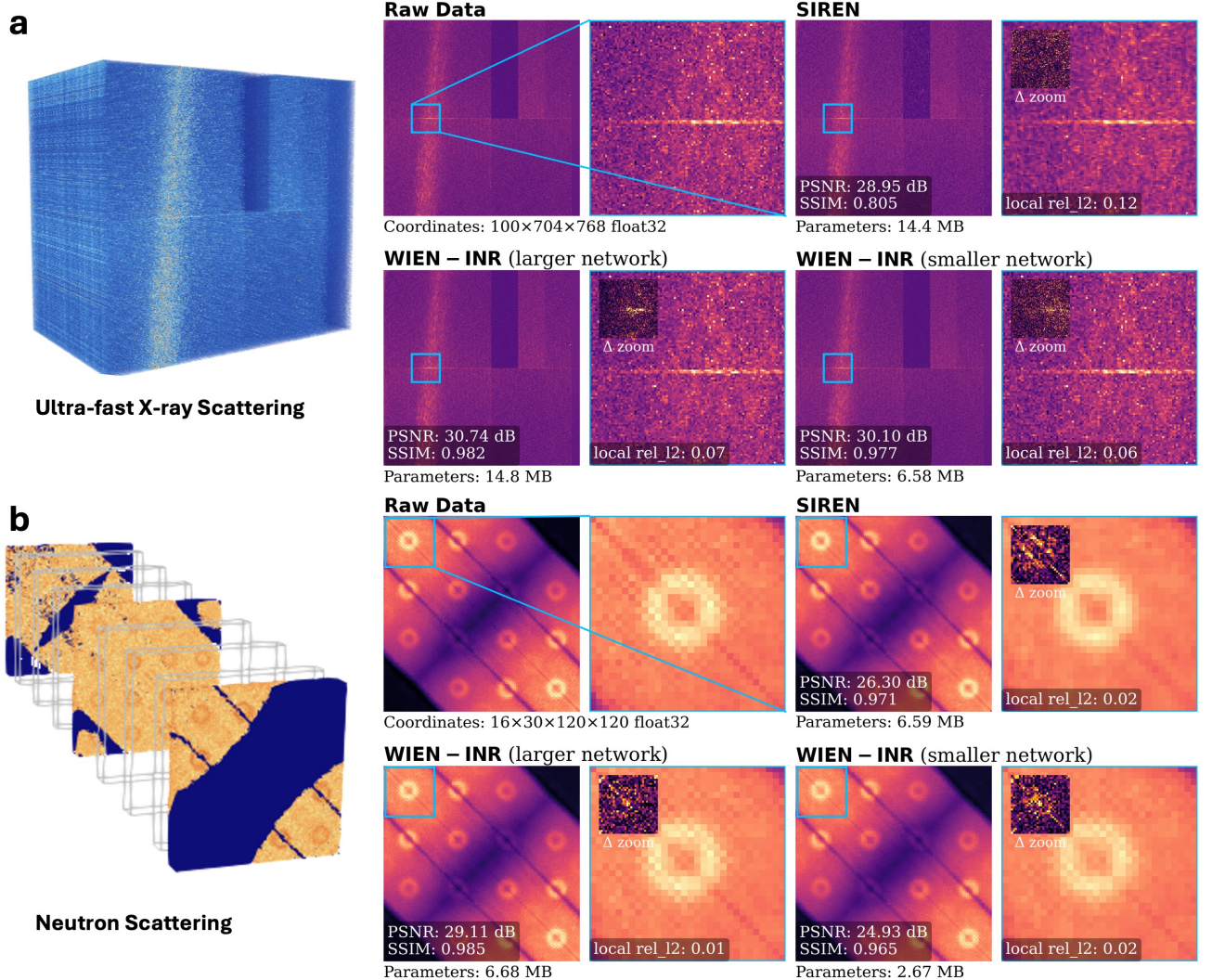


FIG. 5. Compression of volumetric scattering datasets. Results are shown for two distinct datasets, one from ultra-fast X-ray scattering [26] and one from neutron scattering [27]. Each volume is encoded and decoded; Shown on the right are representative 2D slices with zoomed-in regions. In these experiments, speckles constitute the signal of interest, whereas in many other imaging fields they are treated as noise and removed. Zoomed views highlight that SIREN—the strongest baseline—over-smooths speckles in the X-ray data and distorts textures in the neutron data, whereas WIEN-INR remains robust across both cases, preserving high-frequency detail and texture with fewer parameters.

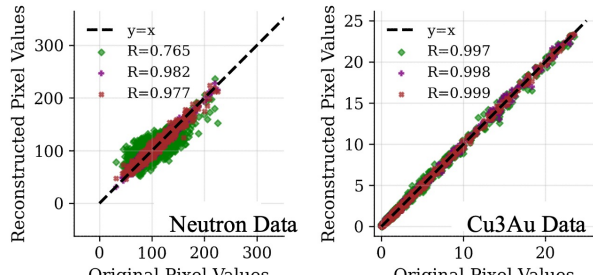
dow size n_r (Fig. 7). We find $J = 4$ provides the best balance of frequency separation, while performance remains stable across wavelet bases, with Haar at $J = 4, n_r = 3$ yielding strong results across all benchmark datasets.

V. FURTHER DISCUSSIONS

Our method demonstrated competent performance in achieving more efficient and accurate scientific data representation with a compact network. Meanwhile, further improvements could be made in network compression and weight quantization. In our experiments, we applied a simple post-training quantization of network

weights (division by two) to reduce memory cost. More sophisticated approaches from the model compression literature could be explored in future work, including the deep compression pipeline and quantization-aware training methods that optimize for rate-distortion under low-precision arithmetic [28–30]. Beyond quantization, structured pruning and sparsification techniques may provide further reductions in model size [31].

Further speedup. As the loss is separable across scales, each subnetwork can in principle be trained independently. The only exception is at the finest scale, where the enhancement network depends on the output of the previously trained subnetwork. This structure allows for a parallelized implementation, which would drastically



Pixel-wise difference of the reconstruction.

FIG. 6. Results are shown for the neutron scattering [27] (left column) and wide-angle X-ray diffraction (right column). Pixel-wise comparison of reconstructed versus ground-truth intensities, where the line $y = x$ indicates perfect reconstruction. The inset reports R , the pixel-wise correlation coefficient between reconstruction and ground truth. Colored scatter plots correspond to SIREN (green), Wavelet-INR (purple), and WIEN-INR (red), respectively.

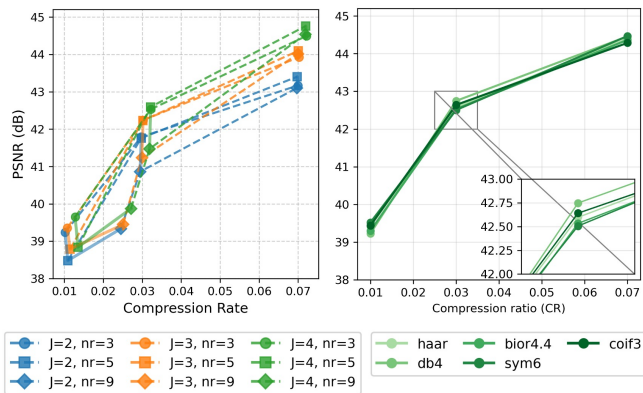


FIG. 7. Robustness to wavelet choices. (Left) Rate-distortion curves for Cu₃Au data using different multi-resolution depths $J \in \{2, 3, 4\}$ and neighborhood sizes $n_r \in \{3, 5, 9\}$ for the refinement module. Colors indicate different J , markers indicate different n_r ; curves with the same n_r are connected by dashed lines, and curves with the same J by solid lines. (Right) Rate-distortion curves for $J = 4$, $n_r = 3$, where our network is trained to encode DWT coefficients computed with five different wavelet bases.

reduce overall training time, with the runtime effectively dominated by the training of the next finest scale and the enhancement step. Additionally, in the context of INR-based representations, where encoding is traditionally slow, recent advances such as divide-and-conquer strategies, meta-learning, and block-wise training [32, 33] have significantly accelerated training, making compression-aware INR frameworks increasingly practical.

Learnable transformations. Alternatively to hand-crafted wavelet transforms, one could learn the transform itself in a data-driven way, turning the framework into a dictionary-learning approach. Promising di-

rections include parameterizing the lifting filters with small networks under perfect-reconstruction constraints, training shallow autoencoders to discover orthogonal wavelet bases, or making scattering/wavelet banks partially learnable to adapt to the data [24, 34]. Finally, one can also explore parameterized analytic wavelet families or even architectures that bypass a fixed transform altogether. For example, Kolmogorov–Arnold Networks (KANs) [35] are a flexible, data-adaptive multi-scale transform that could bypass the need for a fixed basis while retaining interpretability.

Generative framework. Since the current method is designed for faithful, compressive memorization of data, another promising extension is into the generative setting. Particularly, the coarse-to-fine refinement naturally enables super-resolution by predicting fine-scale details from coarser representations, which we leave for future work. Additionally, wavelet-domain diffusion models have shown how coarse-to-fine decomposition can guide generative synthesis of 3D shapes [36], while generative neural fields based on mixtures of implicit functions enable efficient sampling of new signals [37]. In a similar spirit, our multi-resolution plus enhancement structure could be adapted to learn priors over coarse INR representations and enhancement kernels, enabling synthesis of high-fidelity, resolution-scalable scientific data.

Data normalization. In all experiments, we limited preprocessing to a single step — normalizing raw data to the range (0,1) — to preserve the generality of the method. For approximately uniform intensity distributions, we applied min–max normalization. For highly skewed distributions (e.g., strong peak-to-background contrast), we used a $\log(1 + y)$ transform followed by max normalization. While this minimal strategy ensures broad applicability, more tailored preprocessing schemes, adapted to the statistics of specific experiments, could help training and improve reconstruction accuracy.

VI. CONCLUSION

We presented WIEN-INR for scientific data representation, designed to retain the finest details while achieving competitive compression performance among INRs. Our contribution to this area of research is threefold. (1) **Multi-resolution decomposition and finest scale enhancement:** By leveraging wavelet transforms and the enhancement module, the method naturally separates frequency content, enabling efficient learning of more spectrally controlled data representations that are often lost in conventional INRs. (2) **Flexible architecture:** Each wavelet band is represented by an independent subnetwork, with enhancement modules applied selectively to scales where naive INRs are insufficient. This provides both scalability (wavelets can be computed in patches), parallelism (subnetworks can be trained independently), and control (users may choose how many bands to preserve). Additionally, per-pixel accuracy can be set by

choosing an appropriate error bound tolerance through various loss functions such as MAE, MSE, SSIM, or perceptual losses. (3) **Data-agnostic applicability:** The framework operates directly on the wavelet coefficients of raw data with minimal pre-processing and generalizes across diverse scientific modalities, from diffraction patterns to volumetric fields, without tailoring to a specific domain. This multi-resolution framework is particularly suitable for physics applications, as multi-scale decomposition reveals features at different levels of granularity—enabling coarse-to-fine analysis of physically meaningful structures. The decoding stage is nearly instantaneous—requiring only a forward neural network evaluation—and naturally supports ROI-based and resolution-scaled representation, allowing users to reconstruct regions of interest at arbitrary resolutions. We expect this method to find broad application across scientific research and data analytics, offering immediate impact not only in advanced data storage and compression, but also in the new capabilities enabled by neural network representations for sophisticated data analysis.

ACKNOWLEDGMENTS

This work was primarily supported by the Department of Energy, Laboratory Directed Research and Development program at SLAC National Accelerator Laboratory, under contract DE-AC02-76SF00515. C.P. was supported by the Department of Energy, Office of Science, Basic Energy Sciences, Materials Sciences, and Engineering Division.

This research used computational resources of the National Energy Research Scientific Computing Center (NERSC), a US Department of Energy Office of Science User Facility located at Lawrence Berkeley National Laboratory operated under contract DE-AC02-05CH11231, using NERSC award BES-ERCAP0026843.

During the preparation of this work, the authors used the large language model ChatGPT by OpenAI in order to refine the language and enhance the readability of this paper. After using this tool, the authors reviewed and edited the content as needed and take full responsibility for all content in this publication.

[1] Matthew Tancik, Pratul P Srinivasan, Ben Mildenhall, Sara Fridovich-Keil, Nithin Raghavan, Utkarsh Singhal, Ravi Ramamoorthi, Jonathan T Barron, and Ren Ng. Fourier features let networks learn high frequency functions in low dimensional domains. *Advances in Neural Information Processing Systems*, 2020.

[2] Vishwanath Saragadam, Daniel LeJeune, Jasper Tan, Guha Balakrishnan, Ashok Veeraraghavan, and Richard G. Baraniuk. WIRE: Wavelet implicit neural representations. In *2023 IEEE/CVF Conference on Computer Vision and Pattern Recognition (CVPR)*, 2023. doi:10.1109/CVPR52729.2023.01775.

[3] Vincent Sitzmann, Julien Martel, Alexander Bergman, David Lindell, and Gordon Wetzstein. Implicit neural representations with periodic activation functions. In *Advances in Neural Information Processing Systems*, volume 33, pages 7462–7473. Curran Associates, Inc., 2020.

[4] Jana Thayer, Zhantao Chen, Richard Claus, D. Damiani, Christopher Ford, M. Dubrovin, Victor Elmir, W. Kroeger, Xiang Li, S. Marchesini, Valerio Mariani, Riccardo Melchiori, Silke Nelson, Ariana Peck, A. Perazzo, F. Poitevin, Christopher P. O’Grady, Julieth Otero, Omar Quijano, Murali Shankar, M. Uervirojnakorn, Riccardo Veraldi, Matthew Weaver, C. Weninger, Seshu Yamajala, Cong Wang, and Chun Hong Yoon. Massive scale data analytics at LCLS-II. *EPJ Web of Conferences*, 2024. doi:10.1051/epjconf/202429513002.

[5] Egor Sobolev, Philipp Schmidt, Janusz Malka, David Hammer, Djelloul Boukhelef, Johannes Möller, Karim Ahmed, Richard Bean, Ivette Jazmín Bermúdez Macías, Johan Bielecki, and et al. Data reduction activities at European XFEL: Early results. *Frontiers in Physics*, 12, Feb 2024. doi:10.3389/fphy.2024.1331329.

[6] Amer Essakine, Yanqi Cheng, Chun-Wun Cheng, Lipei Zhang, Zhongying Deng, Lei Zhu, Carola-Bibiane Schönlieb, and Angelica I Aviles-Rivero. Where do we stand with implicit neural representations? a technical and performance survey, 2025. URL <https://arxiv.org/abs/2411.03688>.

[7] Yuzhe Lu, K. Jiang, J. Levine, and M. Berger. Compressive neural representations of volumetric scalar fields. *Computer Graphics Forum*, 40, 2021. doi:10.1111/cgf.14295.

[8] Yannick Strümpler, Janis Postels, Ren Yang, Luc Van Gool, and Federico Tombari. Implicit neural representations for image compression. In Shai Avidan, Gabriel Brostow, Moustapha Cissé, Giovanni Maria Farinella, and Tal Hassner, editors, *Computer Vision – ECCV 2022*, pages 74–91, Cham, 2022. Springer Nature Switzerland. ISBN 978-3-031-19809-0.

[9] Thomas Müller, Alex Evans, Christoph Schied, and Alexander Keller. Instant neural graphics primitives with a multiresolution hash encoding. *ACM Transactions on Graphics (TOG)*, 41:1 – 15, 2022. URL <https://api.semanticscholar.org/CorpusID:246016186>.

[10] Ben Mildenhall, Pratul P. Srinivasan, Matthew Tancik, Jonathan T. Barron, Ravi Ramamoorthi, and Ren Ng. NeRF: Representing scenes as neural radiance fields for view synthesis. In Andrea Vedaldi, Horst Bischof, Thomas Brox, and Jan-Michael Frahm, editors, *Computer Vision – ECCV 2020*, pages 405–421, Cham, 2020. Springer International Publishing. ISBN 978-3-030-58452-8.

[11] Thomas M. Cover and Joy A. Thomas. *Elements of Information Theory*. Wiley-Interscience, 2 edition, 2006. doi:<https://doi.org/10.1002/047174882X.ch10>.

[12] Soonbin Lee, Jong-Beom Jeong, and Eun-Seok Ryu. Entropy-constrained implicit neural representations for deep image compression. *IEEE Signal Processing Letters*, 30:663–667, 2023. doi:10.1109/LSP.2023.3279780.

[13] George V. Cybenko. Approximation by superpositions of a sigmoidal function. *Mathematics of Control, Signals and Systems*, 2:303–314, 1989. doi:10.1007/BF02549243.

nals and Systems, 2:303–314, 1989. URL <https://api.semanticscholar.org/CorpusID:3958369>.

[14] Danzel Serrano, Jakub Szymkowiak, and Przemyslaw Musialski. HOSC: A periodic activation function for preserving sharp features in implicit neural representations, 2024. URL <https://arxiv.org/abs/2401.10967>.

[15] Franck Cappello, Allison Baker, Ebru Bozda, Martin Burtscher, Kyle Chard, Sheng Di, Paul Christopher O Grady, Peng Jiang, Shaomeng Li, Erik Lindahl, Peter Lindstrom, Magnus Lundborg, Kai Zhao, Xin Liang, Masaru Nagaso, Kento Sato, Amarjit Singh, Seung Woo Son, Dingwen Tao, Jiannan Tian, Robert Underwood, Kazutomo Yoshii, Danylo Lykov, Yuri Alexeev, and Kyle Gerard Felker. Lossy compression of scientific data: Applications constraints and requirements, 2025. URL <https://arxiv.org/abs/2503.20031>.

[16] Stephane Mallat. *A Wavelet Tour of Signal Processing, Third Edition: The Sparse Way*. Academic Press, Inc., USA, 3rd edition, 2008. ISBN 0123743702.

[17] J.M. Shapiro. Embedded image coding using zerotrees of wavelet coefficients. *IEEE Transactions on Signal Processing*, 41(12):3445–3462, 1993. doi:10.1109/78.258085.

[18] Zhen Liu, Hao Zhu, Qi Zhang, Jingde Fu, Weibing Deng, Zhan Ma, Yanwen Guo, and Xun Cao. FINER: Flexible spectral-bias tuning in implicit neural representation by variable-periodic activation functions. In *Proceedings of the IEEE/CVF Computer Vision and Pattern Recognition Conference (CVPR)*, 2024.

[19] Amirhossein Kazerouni, Reza Azad, Alireza Hosseini, Dorit Merhof, and Ulas Bagci. InCode: Implicit neural conditioning with prior knowledge embeddings. In *Proceedings of the IEEE/CVF Winter Conference on Applications of Computer Vision (WACV)*, pages 1298–1307, 2024.

[20] Kexuan Shi, Xingyu Zhou, and Shuhang Gu. Improved implicit neural representation with fourier reparameterized training. In *Proceedings of the IEEE/CVF Conference on Computer Vision and Pattern Recognition*, pages 25985–25994, 2024.

[21] Rizal Fathony, Anit Kumar Sahu, Devin Willmott, and J Zico Kolter. Multiplicative filter networks. In *International Conference on Learning Representations*, 2021. URL <https://openreview.net/forum?id=0mtmcPkhhT>.

[22] Chang Yu, Yisi Luo, Kai Ye, Xile Zhao, and Deyu Meng. Cross-frequency implicit neural representation with self-evolving parameters, 2025. URL <https://arxiv.org/abs/2504.10929>.

[23] David S. Taubman and Michael W. Marcellin. *JPEG2000: Image Compression Fundamentals, standards, and Practice*. Springer Science + Business Media, LLC, 2013.

[24] R.R. Coifman and M.V. Wickerhauser. Entropy-based algorithms for best basis selection. *IEEE Transactions on Information Theory*, 38(2):713–718, 1992. doi:10.1109/18.119732.

[25] Yuan Ni, Zhanhao Chen, Alexander N. Petsch, Edmund Xu, Cheng Peng, Alexander I. Kolesnikov, Sugata Chowdhury, Arun Bansil, Jana B. Thayer, and Joshua J. Turner. Physics-guided dual implicit neural representations for source separation, 2025. URL <https://arxiv.org/abs/2507.05249>.

[26] Hongwei Chen et al. Testing the data framework for an AI algorithm in preparation for high data rate X-ray facilities. In *4th Annual Workshop on Extreme-scale Experiment-in-the-Loop Computing*, 10 2022. doi:10.1109/XLOOP56614.2022.00006.

[27] AN Petsch, NS Headings, D Prabhakaran, AI Kolesnikov, CD Frost, AT Boothroyd, R Coldea, and SM Hayden. High-energy Spin Waves in the Spin-1 Square-lattice Antiferromagnet La_2NiO_4 . *Physical Review Research*, 5(3):033113, 2023. URL <https://doi.org/10.1103/PhysRevResearch.5.033113>.

[28] Song Han, Huizi Mao, and William J. Dally. Deep compression: Compressing deep neural network with pruning, trained quantization and huffman coding. *International Conference on Learning Representations (ICLR)*, 2016. URL <https://api.semanticscholar.org/CorpusID:2134321>.

[29] Chuxi Yang, Yan Zhao, and Shigang Wang. Deep image compression in the wavelet transform domain based on high frequency sub-band prediction. *IEEE Access*, 7: 52484–52497, 2019. doi:10.1109/ACCESS.2019.2911403.

[30] Y. Lu, K. Jiang, J. A. Levine, and M. Berger. Compressive neural representations of volumetric scalar fields. *Computer Graphics Forum*, 40(3), 06 2021. ISSN ISSN 0167-7055. doi:10.1111/cgf.14295.

[31] Torsten Hoefer, Dan Alistarh, Tal Ben-Nun, Nikoli Dryden, and Alexandra Peste. Sparsity in deep learning: pruning and growth for efficient inference and training in neural networks. *Journal of Machine Learning Research*, 2021.

[32] Jun Han and Fan Yang. DCINR: a divide-and-conquer implicit neural representation for compressing time-varying volumetric data in hours. *IEEE transactions on visualization and computer graphics*, PP, 2025. doi:10.1109/TVCG.2025.3564255.

[33] Runzhao Yang, Tingxiong Xiao, Yuxiao Cheng, J. Suo, and Qionghai Dai. TINC: Tree-structured implicit neural compression. *2023 IEEE/CVF Conference on Computer Vision and Pattern Recognition (CVPR)*, pages 18517–18526, 2022. doi:10.1109/CVPR52729.2023.01776.

[34] Jun-Jie Huang and Pier Luigi Dragotti. WINNet: Wavelet-inspired invertible network for image denoising. *Trans. Img. Proc.*, 31, 2022. ISSN 1057-7149. doi:10.1109/TIP.2022.3184845. URL <https://doi.org/10.1109/TIP.2022.3184845>.

[35] Ziming Liu, Yixuan Wang, Sachin Vaidya, Fabian Ruehle, James Halverson, Marin Soljačić, Thomas Y. Hou, and Max Tegmark. KAN: Kolmogorov–arnold networks. In *International Conference on Learning Representations (ICLR)*, 2025. URL <https://openreview.net/forum?id=0zo7qJ5vZi>. Oral.

[36] Ka-Hei Hui, Ruihui Li, Jingyu Hu, and Chi-Wing Fu. Neural wavelet-domain diffusion for 3D shape generation. December 2022.

[37] Tackgeun You, Mijeong Kim, Jungtaek Kim, and Bo-hyung Han. Generative neural fields by mixtures of neural implicit functions, 2023. URL <https://arxiv.org/abs/2310.19464>.